PAN
ARCHIVES OF ACOUSTICS
Vol. **46**, No. 2, pp. 313–322 (2021)
DOI: 10.24425/aoa.2021.136585

Research Paper

Experimental and Numerical Acoustoelectric Investigation of the New SAW Structure with (RR)-P3HT Polymer in DMMP Detection

Tomasz HEJCZYK[(1)*], Jarosław WROTNIAK[(2)], Mirosław MAGNUSKI[(2)], Wiesław JAKUBIK[(3)]

[(1)] *The Academy of Creative Development – the Foundation*
Marklowice, Poland
[*]Corresponding Author e-mail: fundacja.ark@gmail.com

[(2)] *Institute of Electronics*
Silesian University of Technology, Gliwice, Poland

[(3)] *Institute of Physics CSE*
Silesian University of Technology, Gliwice, Poland

(*received October 9, 2019; accepted December 29, 2020*)

This document presents the results of numerical analyses of the SAW gas sensor in the steady state. The effect of SAW velocity changes depending on how the surface electrical conductivity of the sensing layer is predicted. The conductivity of roughness sensing layer above the piezoelectric waveguide depends on the profile of the diffused gas molecule concentration inside the layer.

Numerical results for the gas DMMP (CAS Number 756-79-6) for layer (RR)-P3HT in the steady state are shown. The main aim of the investigations was to study the thin film interaction with target gases in the SAW sensor configuration based on diffusion equation for polymers. Numerical results for profile concentration in steady state are shown.

The results of numerical acoustoelectric analysis (NAA) allow to select the sensor design conditions, including the morphology of the sensor layer, its thickness, operating temperature and layer type. The numerical results based on the code written in Python, are described and analyzed. The theoretical results were verified and confirmed experimentally.

Keywords: gas sensor; numerical modeling; SAW gas sensor; Ingebrigtsen's formula; DMMP; (RR)-P3HT; numerical acoustoelectric analysis (NAA).

1. Introduction

The main aim of the investigation was to study the thin film interaction with target gases in the SAW sensor based on a simple reaction-diffusion equation (Matsumaga *et al.*, 2001; 2003). Diffusion equations provide theoretical bases for the analysis of physical phenomena like heat transport or mass transport in porous, roughness substrate. The paper summarises the acoustoelectric theory, i.e. Ingebrigtsen's formula (Auld, 1973), dynamics gas diffusion concentration profiles in steady state, and predicts in steady steps the influence of the thin polymer sensor layer with new polymer gas diffusion model on the SAW wave velocity in a piezoelectric acoustic waveguide (Hejczyk *et al.*, 2016).

The most important goals and assumptions of work are:

- The investigations and study of the thin film (RR)-P3HT interaction with target gas DMMP in the SAW sensor configuration based on a simple reaction-diffusion equation (time = 0.01) in a response step (steady stage) (Hejczyk *et al.*, 2015).
- An analitycal design of the model on steady stage (Auld, 1973; Crank, 1975; Matsumaga *et al.*, 2001) of a SAW gas sensor – ineraction polymer (RR)-P3HT on DMMP.

- Optimisation of the construction of the SAW sensor and environmental conditions and investigation of:
  - proper chemical layer,
  - thickness,
  - temperature point of sensor,
  - roughness (Hejczyk *et al.*, 2016).

Delay lines, with acoustic surface wave (AFP), make possible the detection of very small concentrations of chemical compounds in gas mixtures (Wrotniak *et al.*, 2018; Powroźnik *et al.*, 2015). The miniaturization of these transducers resulted in a significant increase in the frequency of AFP sensors.

However, miniaturization of the sensor requires the construction of more complicated or technically advanced electronic devices (Fig. 1), while the test and measurement system for gas detection (Wrotniak *et al.*, 2018; Powroźnik *et al.*, 2015; Hejczyk *et al.*, 2016; Pustelny *et al.*, 2012; Kawalec, Pasternak, 2008; Jasek *et al.*, 2012; Pasternak, 2008) have been designed and developed independently.

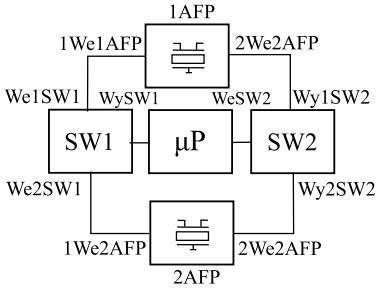

Fig. 1. Measurement system (Patent no. PL 230526 B1 scheme) – System for detecting chemical compounds in gaseous atmospheres, with a sensor using surface acoustic waves (SAW) (Magnuski, Wrotniak, 2018), µP – microprocessor system based on Atmega2560 processor.

The measurement system in Fig. 1 is a module with a double delay line for Rayleigh type AFP. 1AFP is a measuring system with a polymer layer exposed to the tested gas or chemical compound. 2AFP is the reference system line – without a sensor layer. 1AFP and 2AFP are delay lines, switched by means of SW1 and SW2 switches in the G generator feedback loop (Fig. 2) (Magnuski, Wrotniak, 2018). The generator loop is created from cascade connection: the first electronic switch (SW1), a multi-state phase shifter, a broadband amplifier that includes the microprocessor system, and the second electronic (SW2) switch. The system uses a microprocessor system based on the Atmega2560 processor.

The measurement system in Fig. 1 consists of two measuring transducers (1AFP) and (2AFP) made on a common ground, two electronic switches: the first electronic switch (SW1) with two inputs (We1SW1)

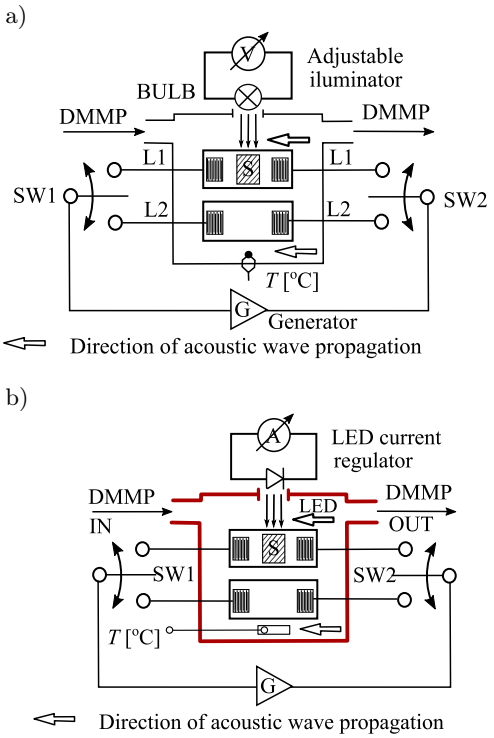

Fig. 2. Measurement system (incandescent lighting): a) light bulb, b) LED lighting (Wrotniak *et al.*, 2018).

and (We2SW1) and one output (WySW1), and a second switch electronic (SW2) with two outputs (Wy1SW2) and (WySWP2) and one input (WeSW2). The first entry gate (We1SW1) of the first switch (SW1) is connected to the first gate (1We1AFP) of the first transducer (1AFP), the second entry gate (We2SW1) of the first switch (SW1) is connected to the first gate (1We2AFP) of the second transducer (2AFP). The first output gates (Wy1SW2) of the second switch (SW2) are connected to the second gates (2We2AFP) of the first transducer (1AFP), the second output gates (Wy2SW2) of the second switch (SW2) are connected to the second gates (2We2AFP) of the second transducer (2AFP) (Magnuski, Wrotniak, 2018).

In order to induce oscillations on the crystal surface, the generator G switches into the loop of the excitation system using switches SW1 and SW2.

The measurement system uses a proprietary single excitation path with a programmable phase shifter matching any sensor line from AFP to the oscillation conditions of the generator loop. Due to the adopted solution of single excitation of each line separately, the switching of the generator circuit between two lines from AFP was used during measurements. The circuit switching was carried out by means of the Atmega2560 microcontroller, whose task is also to set the correct phase shift for the excited channel. The flow direction of the acoustic surface wave signal is schematically shown in Figs 2a and 2b.

In gas sensors from AFP, the mechanism of detecting the concentration of gas or vapours of a chemical compound depends on the interaction of its molecules with a properly selected sensitive sensor layer sensitive to its presence (Yoo *et al.*, 2015). The processes of interaction between gas molecules with layer are kinetic phenomena, mainly sorption (in volume) and adsorption (on the surface), resulting from entrapment of the molecule in the layer or on its surface. The sorption of gas or vapour molecules through the sensor layer causes a change in its mass and electrical conductivity (a change in conductivity affects the change of SAW propagation velocity) which in the measurement system leads to a change in the generator's operating frequency (Auld, 1973). The channel with the sensor layer as a result generates oscillations with a different frequency (usually lower) and is shifted in phase relative to the signal generated in the reference path. The work focuses on the electric effect (Hejczyk *et al.*, 2015).

Figure 2 has been changed to include a light bulb description. The idea of measuring the acoustic wave speed is to measure the frequency of the acoustic wave, exactly the frequency difference between the L1 measurement track and the L2 reference track. Figure 2 schematically shows the measurement system, but the whole system is in the generator's feedback loop. In this system the direction of sound wave propagation is marked as a signal. In the measurement system implemented by the microprocessor system, a phase shifter is connected to the input of the broadband amplifier, the phase shifter is preceded by the SW1 switch. The generator output (G) is connected to SW2 switch.

The results of the research on the application of (RR)-P3HT (poly 3-hexylthiophene regioregular type) produced by means of air spraying on a module with SAW 205 MHz to detect traces of DMMP (Dimethyl methylphosphonate) molecules are presented. DMMP (Wrotniak *et al.*, 2018; Powrożnik *et al.*, 2015) is a non-toxic substance with a similar chemical structure to sarin (Combat Poisoning Agent). It allows for safe experiments.

Due to the photoconductive properties of the P3HT polymer (Long *et al.*, 2015), the layer was additionally activated by a small white lamp (Fig. 2a) (with a maximum light wave of approx. 750 nm) and different illuminance levels. The sensitivity of the layer in the system with SAW (Lee *et al.*, 2011) to the presence of DMMP in this manner was increased. Oscillations (in reference and measurement line) were excited. Generator 205 MHz with switched channels was used.

The essence of the conducted research is the search for new materials and ways to activate them in order to detect trace concentrations of DMMP in the air without the need to apply high temperatures (above 100°C).

2. Analytical model of a gas sensor

In order to optimize the structure of the sensor it is important to get an analytical model of the SAW sensor. The intensity interaction of the electric field with a sensing layer in a surface wave sensor depends not only on the electrical conductivity of the layer, but also on its distance from the piezoelectric waveguide. More details about the analytical model can be found in the paper by Hejczyk *et al.* (2015). Analyzing the acoustoelectric effect in a SAW sensor, the sensing layer was assumed to consist of n-thin sublayers (Fig. 3), in which the concentration of the diffused gas molecules differs but is constant in the respective sublayer.

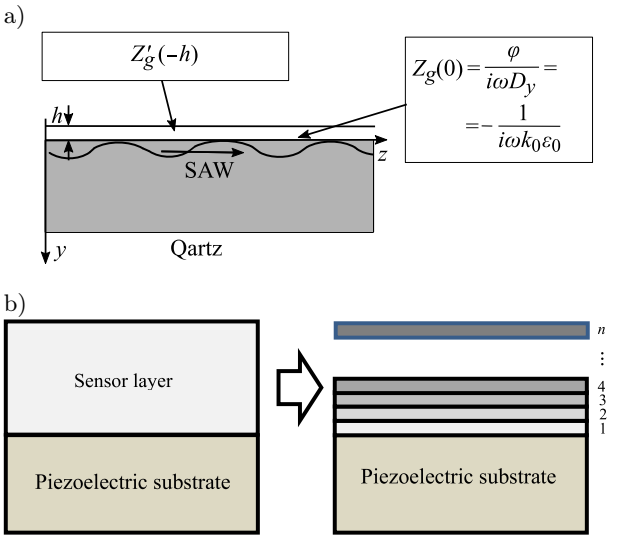

Fig. 3. Exemplary model (a) and equivalent model (b) of the analyzed multilayer sensor structure (Hejczyk *et al.*, 2015).

Of essential importance is the assumption that the electrical conductivity of the respective layers $\sigma(y)$ is proportional to the concentration of the gas molecules C_A in these sublayers:

$$\sigma(y) = \sigma_0 \left(1 + aC_A(y)\right), \tag{1}$$

where σ_0 and a are the conductance of the upper layer and sensitivity parameter, respectively.

In order to obtain an analytical model of a SAW gas sensor, we must find the equivalent electrical impedance on the surface of the piezoelectric waveguide. For this purpose, we apply the law of transformation of the impedance. The impedance of the sublayer at a given distance from the surface of the piezoelectric waveguide is transformed to this surface ($y = 0$). Figure 4 shows a schematic diagram of the action of the impedance transformation law. Using the transformation law for the n-th sublayer, it is possible to calculate the electrical admittance on the surface of the waveguide, which is "seen" by the surface wave.

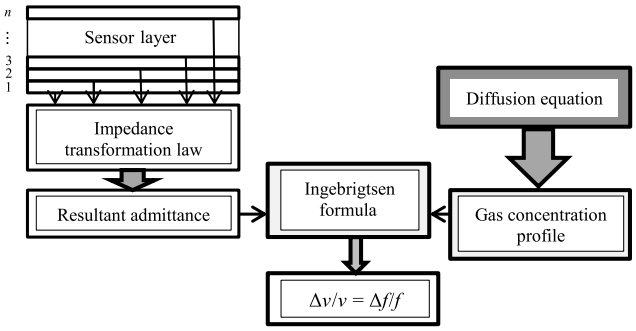

Fig. 4. Analytical diagram of a SAW gas sensor (Hejczyk *et al.*, 2015).

Then, the resultant of the admittance is used in Ingebrigtsen's formula (Auld, 1973) to determine the changes in the velocity of the surface wave resulting from the acoustoelectric interaction between the SAW and the sensor layer with a variable concentration of gas molecules in the y direction (in the depth of the layer).

It can be shown that the Ingebrigtsen formula for n-sublayers takes the following form (Hejczyk *et al.*, 2015):

$$\frac{\Delta v}{v_0} = -\mathrm{Re}\left\{\frac{\Delta k}{k_0}\right\} = -\frac{K^2}{2}\frac{a^*}{a^* + \left[1 + \sum_{i=1}^{n-1} g(y_i, \sigma_{T_2}(y_i))\right]^2 (v_0 C_S)^2}, \quad (2)$$

where

$$a^* = \left[\sigma_{T_2}(1 + aC_{\mathrm{A},y=0}) + \sum_{i=1}^{n-1} \sigma_{T_2}(y_i) f(y_i, \sigma_{T_2}(y_i))\right]^2,$$

n – number of sublayers and $C_S = \varepsilon_0 + \varepsilon_p^T$, $\sigma_{T_2} = \sigma_{T_1} \exp\left(\frac{E_g}{2k_\mathrm{B}} \cdot \frac{T_2 - T_1}{T_1 T_2}\right)$, $T_1 = 300$ K, $\sigma_{T_1} = \sigma_0$, k_B – Boltzman constant, E_g – band gap energy, ε_0 and ε_p^T are respectively, dielectric permittivity of the vacuum and piezoelectric substrate (upper subscript T means in constant stress condition)

$$f(y_i, \sigma(y_i)) = \frac{1 - [\mathrm{tgh}(ky_i)]^2}{[1 + \mathrm{tgh}(ky_i)]^2 + \left[\mathrm{tgh}(ky_i) \cdot \frac{\sigma(y_i)}{\varepsilon_0 v_0}\right]^2}, \quad (3)$$

$$g(y_i, \sigma(y_i)) = \frac{[1 + \mathrm{tgh}(ky_i)]^2 + \mathrm{tgh}(ky_i) \cdot \left(\frac{\sigma(y_i)}{\varepsilon_0 v_0}\right)^2}{[1 + \mathrm{tgh}(ky_i)]^2 + \left[\mathrm{tgh}(ky_i) \cdot \frac{\sigma(y_i)}{\varepsilon_0 v_0}\right]^2}, \quad (4)$$

and $\sigma(y_i) = \sigma_0 [1 + a \cdot C_A(y_i)]$, v_0 – SAW velocity, k – wave number ($k = 2\pi/\lambda$).

The thickness of the layer affects the response of the sensor layer, also in this case. In our case, we identified the height of the layer with the average radius of the sensor layer profile. This is a particularly favourable circumstance because in the perturbation theory the concept of surface conductivity is used. The following graph was obtained by equating the average radius of the R_a layer with the thickness of the layer $\sigma_S = \sigma \cdot R_a$. The mechanical properties of materials by specialists in the domain of mechanics were tested (Gąsiorek, 2013; Gąsiorek *et al.*, 2013; 2018). This fact led us to the development of a mathematical model which takes roughness into consideration. In this case, most of the volume of the layer is close to the surface of the piezoelectric layer of the quartz based. The diffusion of larger molecules is not difficult, however, in layers of greater thicknesses – above about 650 nm, the interaction is not as strong as in smaller ones, eg. 100 nm. The electrical conductivity of the deeper parts of the layer changes, and their contribution to the sensor response is significant. In the case of sensors based on polymer layers, the shape of the surface and its roughness are significant. The above characteristics of the sensor response depending on the average radius of the layer's profile is shown in Fig. 14. The average radius of the R_a layer profile by the height of the H-layer for better presentation was normed (R_a/H – Fig. 14). In the case of the average profile radius R_a of 0, the layer "disappears", boundary conditions correspond to the lack of interaction of the analyte with the sensor layer. When the average radius of the R_a is maximal – layer profile reaches the height of the maximum H. This is a theoretical case when we can obtain an ideal sensor layer in the image of a "rectangular" – and the surface that is not rough – a theoretical case. Therefore, the roughness decides about the response of the DMMP gas sensor based on the optic layer using (RR)-P3HT and this aspect will be developed in further studies. In the case of DMMP, the optimal layer thickness is approx. 100 nm. This thickness is similar to Nioban Lithu ($LiNH_3$) layer and interaction with gases H_2, CO_2, NO_2, NH_3. As a rule, the diffusion of larger molecules is difficult, additional in layers of higher thicknesses, the entire volume of the layer does not saturate. However, in the case of polymers it is the other way round. The electrical conductivity of the deeper parts of the layer also changes, so their contribution to the sensor response is significant. This state describes the solution of the general diffusion equation for polymers (Crank, 1975).

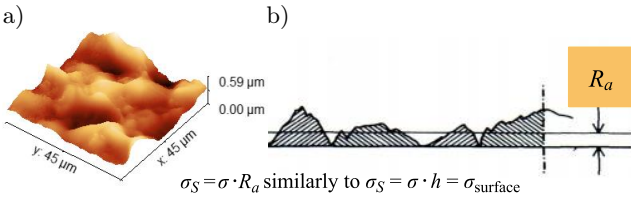

Fig. 5. 3D-AFM view high magnification layer (RR)-P3HT: a) the polymer surface, b) graphic illustration of the average profile radius.

3. Technology of applying the sensor layer

The sensor layer (Fig. 6) of the (RR)-P3HT type polymer with a thickness of ~350 nm, in the empty space of one of the delay lines of the quartz module with AFP was created. The thickness was estimated using the atomic force microscope (AFM) profile analysis. Field fragment polymer plate to use suitably designed mask was exposed. Through an open window the spraying method (nozzle thickness – 0.4 mm) a pre-prepared polymer solution (RR)-P3HT was applied. Compressed synthetic air at a pressure 1 atm. was used. Solution by dissolving about 1 mg (RR)-P3HT in 1 ml chloroform was prepared. The distance of the nozzle from the substrate during the process was about 40 mm, settling time about 3 s (Wrotniak *et al.*, 2018).

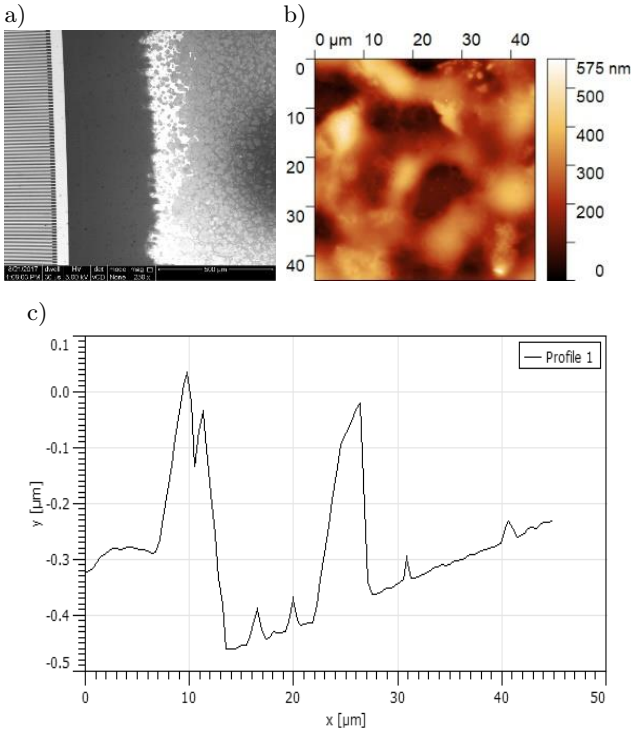

Fig. 6. Layer topography (RR)-P3HT quartz substrate – fragment of polymer layer (RR)-P3HT on quartz crystal from SAW: a) The view of the boundary of a porous layer from the edge of the crystal visible from the top (100×magnification), b) view under magnification, c) profile.

4. Experiment

The main aim of researching of selected structures of the sensor with a surface acoustic wave was an experimental verification of the response of numerical analysis sensor. We must emphasize that performing experimental researches was possible in limits, because of the wide range of work and the complex of technological processes connected with the practical feasibility of the sensor structure (Wrotniak, Magnuski, 2016).

Experimental results are presented in Figs 7–12. The results of reference frequency were normed. The results (in a relative scale) are shown in Figs 11 and 12. The influences of the gas concentration and temperature on relative change of frequency are shown in Figs 11 and 12. A view of SAW sensor is presented in Fig. 7.

Fig. 7. The practical implementation of the invention of the Patent no. PL 230526 B1 – a measuring chamber for testing using SAW sensors.

Experimental results for illuminating LEDs (200 mA) with different wavelengths the layer (RR)-P3HT are presented in Fig. 8. The research system from Fig. 2b was used. The measuring system uses: a light bulb with parameters – 100 lumen 10 W, G4 and diodes – 1 W SMD 350 mA ProLight Opto.

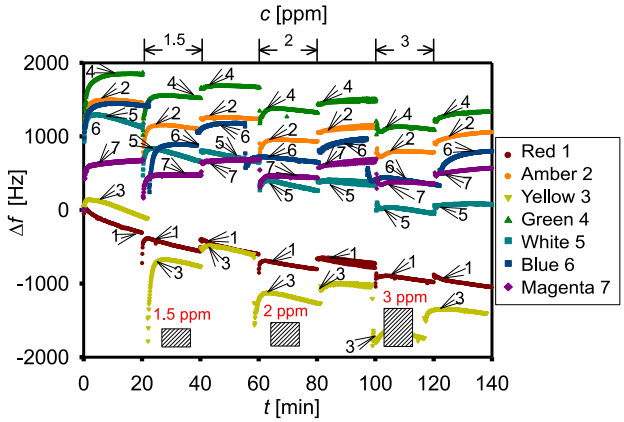

Fig. 8. Experiment – sensor layer (RR)-P3HT, thickness 500 nm, gas DMMP (1.5; 2; 3 ppm, illumination by diode 200 mA (selected wavelengths) relative change of velocity *versus* time (concentration).

Results of measurements DMMP in interaction with polymer layer (RR)-P3HT illuminated with a diode light of 200 mA in the form of a histography are shown in Fig. 9.

The parameters of the LEDs are as follows:

- amber: 58.9–67.2 lm, 587–597 nm,
- magenta: 23.5–30.6 lm, 579–581 nm,
- yellow: 76.6–87.4 lm, 560 nm,
- red: 51.7–58.9 lm, 613.5–631 nm,
- blue: 39.8–51.7 lm, 455–475 nm,
- green: 168.4–192 lm, 530 nm,
- white: 130–140 lm (Fig. 10).

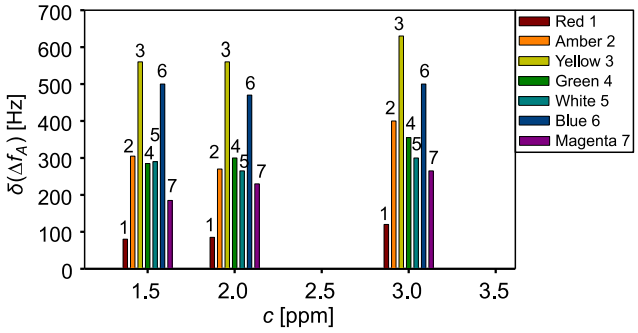

Fig. 9. Experiment – sensor layer (RR)-P3HT, thickness 500 nm, gas DMMP (1.5; 2; 3 ppm, illumination by diode 200 mA (selected wavelengths) – histography – relative change of velocity *versus* time (concentration).

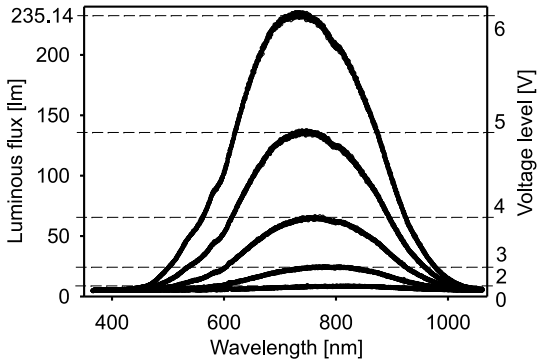

Fig. 10. Example spectral characteristics of the white light source used, determined with a USB 4000 spectrometer for five values of supply voltage 2, 3, 4, 5, and 6 V.

Three measurement series were made. The diodes were driven with 100, 200, 300 mA current. The layer was additionally activated by a small incandescent lamp with white light (with a maximum for about 750 nm) and different illuminance (Fig. 10). Exposure time was about 10 min for each 100, 200, 300 mA current.

In order to optimize numerically and compare the experiment with the theory, the results of the experiment were normalized as follows: Fig. 11 – depending on the concentration, Fig. 12 – depending on the temperature.

For a polymer layer at temperature of ~35.5°C as a result of lighting with a white light source with a 2 V supply voltage (2 ppm DMMP in air) a reduction of the differential frequency Δf to 130 Hz was obtained. Appropriate for the light source supply voltage of approx. 3 V, (temperature ~43.6°C) the decrease in the differential frequency was approx. Δf = −200 Hz, 4 V (temperature ~52°C) Δf = −270 Hz, 5 V (temperature ~62.4°C) Δf = −300 Hz. All results with a DMMP concentration of 2 ppm in air are presented in this work.

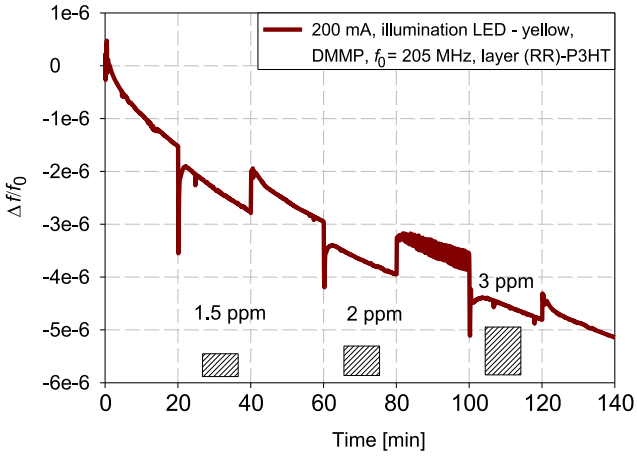

Fig. 11. Experiment – sensor layer (RR)-P3HT, thickness 500 nm, gas DMMP (1.5; 2; 3 ppm, illumination by diode 200 mA (yellow light) normalized results relative change of velocity *versus* time (concentration) – measuring system Fig. 2b.

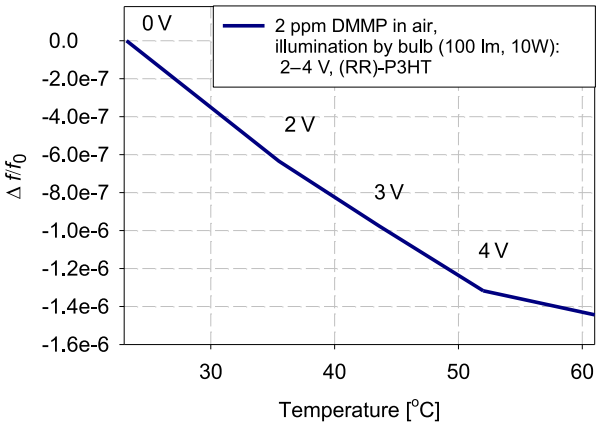

Fig. 12. Experiment – sensor layer (RR)-P3HT, thickness 500 nm, gas DMMP: 2 ppm, illumination by bulb: 2–4 V, relative change of velocity *versus* temperature normalized results – measuring system Fig. 2a.

5. NAA interaction in the sensing layer in the steady state

The roughness of polimer (Crank, 1975) sensor layer for the average height of the layer profile from 0 to 500 nm (max. average height of the layer profile) was theoretically analysed. The morphology of the (RR)-P3HT layer with SAW quartz substrate – made by PhD A. Kaźmierczak-Bałata measured polymer layer is presented. The thickness using the atomic force microscope (AFM) profile analysis was estimated.

For Fig. 13, the analysis for a polymer is performed. For the assumed DMMP gas ambient parameters (temperature, concentration 3 ppm) and layer parameters (sensitivity, conductivity, diffusion parameters, substrate – quartz), the graph shows the value of about $3.98 \cdot 10^{-6}$ for a layer with a thickness of 500 nm. The changes resulting from the numerical model are

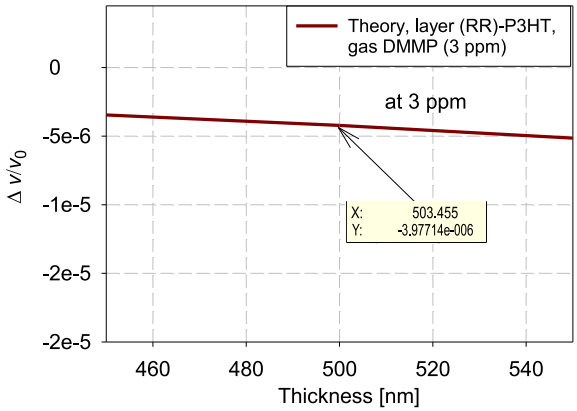

Fig. 13. Relative changes of velocity *versus* thickness from 100 nm to 1800 nm, layer (RR)-P3HT, gas DMMP: a = 1 ppm^{-1}, $\sigma_s = 5 \cdot 10^{-4}$ S, t = 0.01 s, (k = 0 s^{-1}), $D_K = 10^6$ nm^2/s, E_g = 5 eV, M = 124.08 g/mol, concentration: 3 ppm, temperature t = 305 K, $K^2/2$ (quartz) = 0.09%.

at a relative level of changes of the order of 10^{-6} and agree on the order of magnitude from Fig. 11 – experimental studies, where the range of changes is from 0 to $5 \cdot 10^{-6}$.

The concept of roughness was introduced to the theory of SAW sensors with the polymer layer based on an analogy to the concepts found in the perturbative calculus (Auld, 1973), i.e. the radius of the roughness profile can be compared with the height of the sensor layer. This is graphically illustrated in Fig. 14.

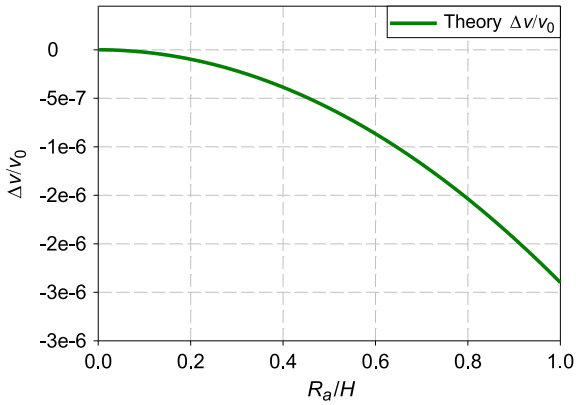

Fig. 14. Relative changes of velocity *versus* roughness, temperature 305 K (32°C), (RR)-P3HT, a = 1 ppm^{-1}, σ_s = $5{\cdot}10^{-4}$ S, $D_K = 10^6$ nm^{2}s^{-1}, E_g = 2.7 eV, M = 124.08 g/mol, DMMP concentration: 2 ppm, thickness 500 nm (H), $K^2/2$ (quartz) = 0.09%, measurement AFM R_a = 76 nm.

The characteristic from Fig. 13 shows the dependence of the radius of roughness R_a normalized to the height of the layer H (change from 0 to 500 nm). Figure 14 illustrates the behaviour of the sensor: there isn't be any interactions gas – sensor layer when R_a roughness = 0, $\Delta V/V_0 = 0$ (no change in relative speed value). The roughness radius R_a = 500 nm of the interaction is maximum approx. $\Delta V/V_0 = 2.9 \cdot 10^{-6}$, but it corresponds to the values of interactions from experimental tests presented in Fig. 11, approx. $\Delta f/f_0 = 3.4 \cdot 10^{-6}$ for a value of 2 ppm (maximum changes in relative value of the acoustic wave velocity).

Figure 15 shows the theoretical dependence of layer interactions on temperature. The graph is not linear, but the theoretical changes that occur when temperature changes show that the theory is consistent with the experiment in the order of magnitude in the first approximation (Fig. 12). The results from Fig. 12 were used because the bulb caused the increase of the temperature in the chamber.

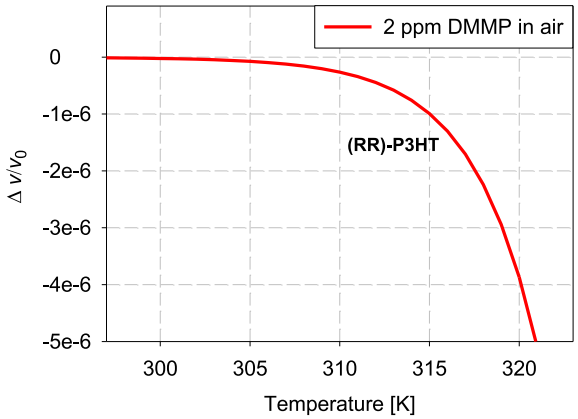

Fig. 15. Temperature adjustment approx. 293–322 K (20–49°C) – theoretical curve resulting from numerical calculations.

The results of experiment were compared to the theory. Figure 15 shows theoretical numerical analysis in the temperature range of about 293–322 K. Below, a comparison of numerical calculations based on the assumed layer model with experimental measurements was made. The calculations for a DMMP concentration of 2 ppm were made. The theoretical curve is the result of numerical calculations matched to the experiment for point of convergence as presented in Fig. 16.

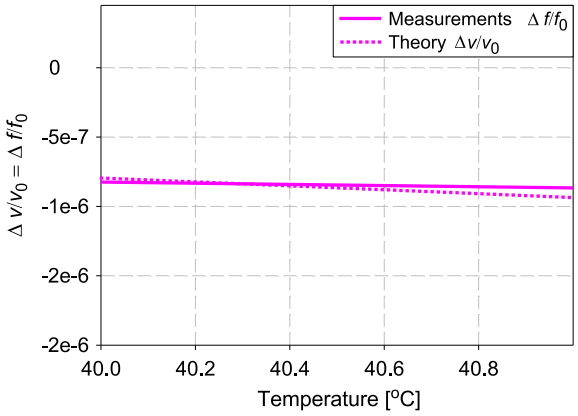

Fig. 16. The theoretical curve resulting from numerical calculations The results of numerical calculation (theory) to experimental research in temperature approx. 40–41°C (point of convergence) were adapted.

In Fig. 17, the theoretical dependence of the sensor response depending on the concentration in the range from 1–3 ppm is presented. The results of the experimental research concerning the concentration of 1.5–3 ppm and at 32°C were investigated. All tests were performed on a piezoelectric substrate made of quartz.

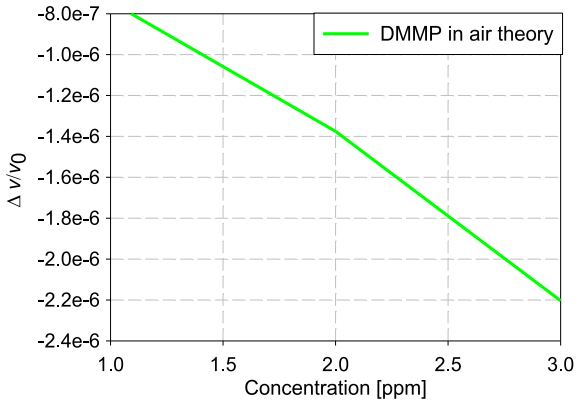

Fig. 17. Relative changes of velocity *versus* concentration, temp. 305 K (32°C), (RR)-P3HT, a = −1.75 ppm^{-1}, σ_s = $5 \cdot 10^{-4}$ S, D_K = 10^6 nm^{2}s^{-1}, E_g = 2 eV, M = 124.08 g/mol, gas DMMP, thickness 500 nm, $K^2/2$ (quartz) = 0.09%.

The theory was compared to the experiment in the scope of the studied concentrations in the drawing below. Very good convergence in the concentration range of 2 ppm DMMP was achieved.

The analysis of interactions in the scope of comparative analysis depending on the concentration is not perfect (Fig. 18), it converges at one point for the value of 2 ppm, but agrees with the order of magnitude from the experiment (Fig. 11).

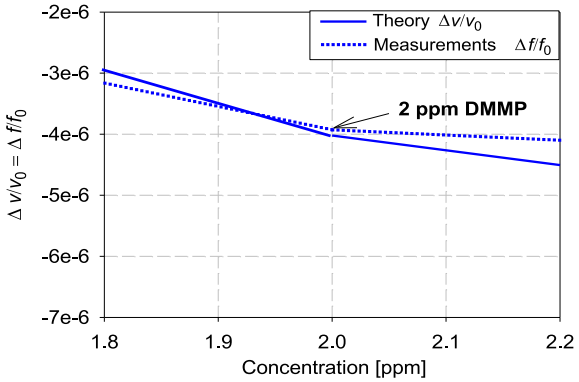

Fig. 18. Relative changes of velocity *versus* concentration, temperature 296 K (23°C), (RR)-P3HT, a = −1.75 ppm^{-1}, σ_s = $5 \cdot 10^{-4}$ S, D_K = 10^6 nm^{2}s^{-1}, E_g = 1.5–2 eV, M = 124.08 g/mol, gas DMMP, thickness 500 nm, $K^2/2$ (quartz) = 0.09%, matching the theory with the experiment.

A simple error analysis was performed. Indeed, the mathematical model does not perfectly approximate all values, but at 2 ppm the error value is minimal. The theoretical mathematical model presents the tendency of acoustic wave velocity changes for the assumed parameters of the sensor layer and the parameters of the layer environment. The theoretical curve shows the trend of changes, i.e. as the gas concentration increases, a change in the speed of the acoustic wave should be expected. The curves agree on an order of magnitude. Good compliance was obtained with a minimum error for one point of 2 ppm for which the relative changes in the frequency of the acoustic wave were maximum. It can be stated that there is a positive correlation between the two graphs, i.e. as the concentration of DMMP gas increases, the frequency of the acoustic wave changes – the speed of the acoustic wave decreases, as indicated by the theoretical model. We would like to emphasize that the model shows very accurately the relative values of velocity changes for concentration values of 2 ppm (in theory) and coincides with the experiment in the detection of trace amounts of DMMP compound vapours (2 ppm) in the air using the AFP method. This is not the exact convergence of the model and data, but it is very accurate in terms of magnitude. However, the model with its complexity (see formulas (2)–(4)) and universality shows tendencies of changes that overlap and agree in practice. The purpose of the work was also to model the sensor behaviour for maximum analyte (DMMP gas) changes, i.e. 2 ppm, and this goal was achieved with a relative error of 2.53%. The characteristics to 2 ppm were narrowed, showing the convergence and interesting part of the numerical analysis (Figs 11 and 18).

6. Summary

Sensor studies of photoconductive (RR)-P3HT were performed as a potential material for detecting trace amounts of DMMP compound vapours (2 ppm) in air with the use of the AFP method. Polymer (RR)-P3HT possesses significant sensitivity to trace amounts of DMMP, only when additional white light was used. Increasing the light flux also causes the sample temperature to rise and to obtain larger frequency variations (130–300 Hz) for the same concentration of 2 ppm DMMP in the air. Estimated response and regeneration times for this DMMP concentration are respectively 10–20 s and 7 min. Extensive NAA of the SAW sensor response depending on parameters like: concentration, roughness, temperature and thickness were conducted. Numerical researches were performed in the steady state. NAA were performed using proprietary software written in Python. The layer thickness decides about the maximum range of the detected gas concentration. Also the choice of the temperature of the polymer sensor is important – the optimal work temperature depends on the type of the sensor layer and its roughness. The change of temperature allows to determine the point of sensor work, and has also an impact on the speed of its response and the recove-

ry time of the sensing properties of the sensor layer (Hejczyk, Urbańczyk, 2013). Experimental results of a SAW sensor with (RR)-P3HT were achieved for three thicknesses of the layers (~100, ~350, ~550 nm) and the same morphology. The main aim was to verify experimentally the analytical model of the SAW gas sensor affected on 2 ppm DMMP in the air. Experimental results confirmed the usefulness of the elaborated analytical model for researches of the SAW sensor in the design stage. In particular, the influence of the concentration and temperature was confirmed. The essential parameter of the polymer sensor is the roughness of the sensing layer.

The results of NAA of the SAW sensors investigations confirmed experimentally are shown. Different sources of light (incandescent from bulbs, LED) were selected and different wavelengths (histogram) were checked.

The study shows that the parameters of the sensor layer for the SAW sensor should be individually adjusted, according to the type of the detected gas and to the applied sensing layer.

The next stage of the work will be an attempt to separate the influence of the applied optical activation from thermal activation, and also to activate the polymer by lighting with LED light of different wavelengths and different light energy and P3HT morphology for material tests (Gąsiorek *et al.*, 2013; 2018) using Abbot-Firestone curves.

The exposure time of polymer layers was also experimentally selected for about 10 min for each current value of 100, 200, 300 mA and the sensor layer was illuminated with LED light of different wavelengths and different light energy. From the tests, the best results for yellow light: 76.6–87.4 lm and wavelength λ = 560 nm were obtained.

Due to the photoconductive properties of the (RR)-P3HT polymer, the layer was additionally activated by a small incandescent lamp with white light (with a maximum characteristic for about 750 nm – Fig. 10) and different illuminance as well as irradiation with light from LEDs of different wavelengths. The essence of the research is to search for new materials and ways to activate them to detect trace concentrations of DMMP vapours in the air without the need for high interaction temperatures (above 100°C).

The authors' main goal was to numerically analyze phenomena based on the experimental research and to create a predictive model that would model the tendency of changes before they appear.

The main assumptions in this part of the work have been achieved:

- Considered boundary electric effect on SAW sensor based on polimer layer (Hejczyk *et al.*, 2018).
- Analytical gas sensor on steady stage based on polimer layer (RR)-P3HT elaborated and presented.
- Numerical results have been shown for concentration DMMP in steady state for (RR)-P3HT layer and compared with experiment.

Acknowledgments

Authors would like to thank the Presidents: Wojciech Wajda WASKO SA and Grzegorz Kamiński ENTE Ltd. for the possibility of work: theoretical, analytical, numerical and research works as well as participation in R&D works financed from the NCBiR grants.

References

1. Auld B.A. (1973), *Acoustic Fields and Waves*, Vol. 2, Wiley, New York, pp. 271–290.
2. Crank J. (1975), *The Mathematics of Diffusion*, Clarendon Press, Oxford, pp. 259–262.
3. Czop P., Gąsiorek D., Gniłka J., Sławik D., Wszołek G. (2012), Fluid-structure simulation of a valve system used in hydraulic dampers, *Modelowanie Inżynierskie*, **14**(45): 197–205.
4. Gąsiorek D. (2013), The application of the smoothed particle hydrodynamics (SPH) method and the experimental verification of cutting of sheet metal bundles using a guillotine, *Journal of Theoretical and Applied Mechanics*, **51**(4): 1053–1065.
5. Gąsiorek D., Baranowski P., Malachowski J., Mazurkiewicz L., Wiercigroch M. (2018), Modelling of guillotine cutting of multi-layered aluminum sheets, *Journal of Manufacturing Processes*, **34**(Part A): 374–388, doi: 10.1016/j.jmapro.2018.06.014.
6. Gąsiorek D., Mężyk A., Skibniewski A., Głuchowski W. (2013), Metallographic investigations of metal plate edges after cutting, *Journal of Achievements in Materials and Manufacturing Engineering*, **60**(1): 31–38.
7. Hejczyk T., Kamiński G., Ogaza R. (2018), *Application of the hybrid sensor with acoustic surface wave* [in Polish: *Zastosowanie hybrydowego sensora z akustyczną falą powierzchniową*], Patent no PL 229696 B1, pp. 2–5.
8. Hejczyk T., Pustelny T., Wszołek B., Jakubik W. (2016), Numerical analysis of sensitivity of SAW structure to the effect of toxic gases, *Archives of Acoustics*, **41**(4): 747–755, doi: 10.1515/aoa-2016-0072.
9. Hejczyk T., Urbańczyk M., Pustelny T., Jakubik W. (2015), Numerical and experimental analysis of the response of a SAW structure with WO3 layers an action of carbon monoxide, *Archives of Acoustics*, **40**(1): 19–24, doi: 10.1515/aoa-2015-0003.
10. Jasek K., Miluski W., Pasternak M. (2011), New approach to saw gas sensors array response measurement, *Acta Physica Polonica A*, **120**(4): 639–641, doi: 10.12693/APhysPolA.120.639.

11. Jasek K., Neffe S., Pasternak M. (2012), SAW sensor for mercury vapour detection, *Acta Physica Polonica A*, **122**(5): 825–828, doi: 10.12693/APhysPolA.120.639.

12. Kawalec A., Pasternak M. (2008), Microwave humidity sensor based on surface acoustic wave resonator with nafion layer, *IEEE Transactions on Instrumentation and Measurement*, **9**(57): 2019–2023.

13. Kawalec A., Pasternak M., Jasek K. (2008), Measurements results of SAW humidity sensor with nafion layer, *European Physical Journal: Special Topics*, **154**: 121–126.

14. Lee H.J., Park K.K., Kupnik M., Oralkan Ö., Khuri-Yakub B.T. (2011), Chemical vapor detection using a capacitive micromachined ultrasonic transducer, *Analytical Chemistry*, **83**(24): 9314–932, doi: 10.1021/ac201626b.

15. Long Y., Wang Y., Du X., Cheng L., Wu P., Jiang Y. (2015), The different sensitive behaviors of a hydrogen-bond acidic polymer-coated SAW sensor for chemical warfare agents and their simulants, *Sensors*, **15**: 18302–18314, doi: 10.3390/s150818302.

16. Magnuski M., Wrotniak J. (2018), *System for detecting chemical compounds in gaseous atmospheres, with a sensor using surface acoustic waves (SAW)* [in Polish: *Układ do wykrywania związków chemicznych w atmosferach gazowych z czujnikiem wykorzystującym akustyczne fale powierzchniowe (AFP)*], Patent no PL 230526 B1.

17. Matsumaga N., Sakai G., Shimonoe K., Yamazoe N. (2001), Diffusion equation-based study of thin film semiconductor gas sensor-response transient, *Sensors and Actuators B*, **83**(1–3): 216–221, doi: 10.1016/S0925-4005(01)01043-7.

18. Matsumaga N., Sakai G., Shimonoe K., Yamazoe N. (2003), Formulation of gas diffusion dynamics for thin film semiconductor gas sensor based on simple reaction-diffusion equation, *Sensors and Actuators B*, **96**(1–2): 226–233, doi: 10.1016/S0925-4005(03)00529-X.

19. Powroźnik P., Jakubik W., Kaźmierczak-Bałata A. (2015), Detection of organophosphorus (DMMP) vapour using phthalocyanine-palladium bilayer structures, *Procedia Engineering*, **120**: 368–371, doi: 10.1016/j.proeng.2015.08.640.

20. Pustelny B., Pustelny T. (2009), Transverse acoustoelectric effect applying in surface study of GaP: Te(111), *Acta Physica Polonica A*, **116**(3): 383–384, doi 10.12693/APhysPolA.116.383.

21. Pustelny T. *et al.* (2012), Gas sensors based on nanostructures of semiconductor ZnO and TiO_2, *Bulletin of the Polish Academy of Sciences: Technical Sciences*, **60**(4): 853–859, doi: 10.2478/v10175-012-0099-1.

22. Sakiewicz P., Nowosielski R., Babilas R., Gąsiorek D., Pawlak M. (2013), FEM simulation of Ductility Minimum Temperature (DMT) phenomenon in CuNi25 alloy, *Journal of Achievements in Materials and Manufacturing Engineering*, **61**(2): 274–280.

23. Wrotniak J., Jakubik W., Powroźnik P., Stolarczyk A., Magnuski M. (2018), Acoustic tests of RR-P3HT type polymer for the detection of DMMP in the air [in Polish: Akustyczne badania polimeru typu RR-P3HT do wykrywania DMMP w powietrzu], *Przegląd Elektrotechniczny*, **94**(6): 70–73, doi: 10.15199/48.2018.06.12

24. Yoo R., Kim J., Song M.J., Lee W., Noh J.S. (2015), Nano-composite sensors composed of single-walled carbon nanotubes and polyaniline for the detection of a nerve agent simulant gas, *Sensors and Actuators B: Chemical*, **209**: 444–448, doi: 10.1016/j.snb.2014.11.137.